AC Impedance Study of NiO$_x$-GDC$_{(1-x)}$ Nanocomposites

A.U. Chavan, L. D. Jadhav, S. Varma, S.R. Bharadwaj

Abstract— The synthesis of nanostructured Gd doped ceria (GDC) and NiO has been reported by a simple and cost effective solution combustion method. The powders were formed at low temperature (~300°C). The NiO$_x$-GDC$_{(1-x)}$ where x = 0.1, 0.2, 0.3, 0.4, 0.5, and 0.6; nano-composites were formed by physical mixing of these nano powders. The grain interior charge transfer mechanism in these nano-composites was confirmed by using impedance spectroscopic measurements in the frequency range from 1 Hz to 10 MHz. The impedance spectroscopic measurements of the composites were examined in the temperature range 100°C-600°C. The grain and grain boundary contributions to the electrical conductivity varied with the composition and temperature. The activation energies for both grain and grain boundary conductivity decreased with increase in NiO content. The study also revealed that 40 % NiO content is a percolation limit for NiO-GDC nano-composites. The effect of NiO addition on relaxation behaviour of these NiO$_x$GDC$_{(1-x)}$ nano-composites is investigated for the first time using impedance measurements.

Index Terms— Electrical properties, Nano-composites, Porosity, Relaxation.

I. INTRODUCTION

Composites have gained substantial interest due to their interesting electrical and magnetic properties and technological applications [1]. Basically electrical composite is a physical mixture of two or more solid phases that possesses mixed conductivity. Therefore, its electrical properties can be tailored by controlling the relative mole fraction of the phases for specific applications. The properties of composites are strongly influenced by the microstructural features such as grain size distribution and morphology, in addition to the electrical properties of each phase. In recent past, composites are widely used in solid oxide fuel cells (SOFCs). For example, composite electrolytes exhibiting mixed H$^+$ and O^{2-} ionic conductivity have better efficiency for direct operation of the hydrocarbon fuel [2]. Composite electrodes exhibiting ionic and electronic conductivity not only increase the length of triple phase boundary but also provides thermal expansion coefficient match with electrolyte hence improves electrode catalytic reactions and thereby fuel cell performance. An electrical composite consisting of ionic and electronic phases are of great importance [1]-[5] in batteries, gas sensors as well as membranes also. Further this kind of nano-composites usually shows conductivity significantly higher than in both of the constituent phases.

An electrical nano-composite NiO-GDC (gadolinium doped ceria), which can be reduced in-situ during the first operation of SOFC [6]-[7] is a suitable anode material for Intermediate Temperature Solid Oxide Fuel Cell (IT-SOFC). NiO acts as good catalyst for oxygen activation [8], and provides good electrical conductivity while GDC mainly acts as matrix to support the catalyst and prohibits the Ni from agglomeration under operating conditions [6]. It also provides better matching of thermal expansion coefficient and suppresses carbon deposition on electrodes in methane rich fuels [9]. The cermet nano-composites can substantially enhance the hydrogen dissociation with reduced electrode polarization resistance, and also increase the TPBs.

In recent years, NiO$_{30}$-GDC$_{70}$ has been exhaustively studied as an anode for the SOFC. But little work can be found on the composite series. In our earlier work, we reported the structural, morphological and dc conductivity studies of solution combustion synthesized NiO$_x$-GDC$_{(1-x)}$ composites, where x = 0.1, 0.2, 0.3, 0.4, 0.5, and 0.6 [10]. Nevertheless, the electrical properties, which were found to vary with varying amounts of the constituent phases, need to be explored. Therefore in present report series of NiO$_x$-GDC$_{(1-x)}$ nanocomposites was intensively studied by impedance spectroscopy. As impedance spectroscopy (IS) is powerful method of characterizing the electrical properties of materials and their interfaces. It is also capable to identify the different relaxation frequencies owing to different charge mechanisms. Park et al [9] have studied ac impedance of NiO-YSZ (yttria stabilized zirconia) but there are no previous studies on the ac impedance spectroscopy as well as relaxation behavior of NiO-GDC nano-composites. In the present work the effect of NiO variation on conduction mechanism in correlation with the relaxation is investigated first time for the series of NiO$_x$-GDC$_{(1-x)}$ nano-composites, where x = 0.1, 0.2, 0.3, 0.4, 0.5, and 0.6.

Dr. Archana Chavan "Postdoctoral Fellow" at Chonnam National University, South Korea

Dr. L. D. Jadhav Assistant Professor at Department of Physics, Rajaram College Kolhapur, Maharashtra, India.

Dr. Salil Varma Scientist-F at Chemistry Division, Bhabha Atomic Research Centre, Trombay, Mumbai - 400085, INDIA.

Prof. S. R. Bharadwaj Senior Scientist Chemistry Division, Bhabha Atomic Research Centre, Trombay, Mumbai - 400085, INDIA.

II. EXPERIMENTAL

For the combustion synthesis of 10 mol% Gd doped ceria (GDC10: Ce$_{0.9}$Gd$_{0.1}$O$_{1.95}$) nanopowder, metal nitrates Ce(NO$_3$)$_3$.6H$_2$O and Gd (NO$_3$)$_3$.6H$_2$O were used as oxidants and glycine (C$_2$H$_5$NO$_2$) as a fuel. The stoichiometric amounts of metal nitrate precursors were dissolved in deionized water [11]-[12]. With the help of burette, fuel was added drop by drop while stirring at room temperature to form homogeneous solution of metal nitrates and fuel. The solution was stirred and heated on a magnetic stirrer for the removal of moisture and hence to form gel. The formed gel was kept on preheated hot plate to combust [13]. The resultant nanopowder of GDC10 was then collected and calcined in air at 600°C for 2h.

to remove any carbon based residues that might have remained in the oxide powder. Similar procedure was repeated to form NiO wherein Ni(NO$_3$)$_2$.6H$_2$O was used as metal nitrate and glycine as fuel. Ash obtained was calcined at 500°C for 2h. The morphology of the particles in ceramic materials is a consequence of the preparation method, and the combustion method favors porous nanoparticles. This method can produce homogeneous powder composed of small and uniform particles. The nano powders of GDC and NiO were characterized by XRD, FTIR and SEM which have been reported in our previous report [10-12].

NiO$_x$-GDC$_{(1-x)}$ where x = 0.1, 0.2, 0.3, 0.4, 0.5, and 0.6 were formed by grinding the nano powders of NiO and GDC in agate mortar for 3h. These nano-composite powders were pressed in the form of cylindrical pellets by applying a uniaxial pressure of 7 tons for three minutes with the help of hydraulic press. The formed pellets have 13mm diameter and 1mm thickness. Extreme care was taken to see that palletization of all the samples was done under identical conditions. All the pellets were pre-sintered at 900°C for 2h and finally sintered at 1000°C for 8h at heating rate of 1°C /min in air atmosphere. The process of pre-sintering gives slow heating of the pellets with removal of carbonaceous products if any, formed during palletization and hence no formation of cracks in the samples during final sintering still at higher temperatures. These nanocomposite samples were named as N1G1, N2G1, N3G1, N4G1, N5G1, N6G1 respectively for x = 0.1, 0.2, 0.3, 0.4, 0.5, 0.6 in NiO$_x$-GDC$_{(1-x)}$.

Structural studies of these samples were carried out by XRD (Phillips-3710 powder X-ray diffractometer) in the 2θ range of 20 - 80° using CuKα1 radiation (λ= 1.54056Å). The XRD patterns were compared with standard JCPDS files of NiO (78-0643; cubic NiO) and GDC10 (75-0161). The conventional Archimedes method was used to measure the density of these samples. The ac electrical conductivity measurements were carried out in air atmosphere with the help of electrochemical impedance spectroscopy in temperature range of 100°C to 600°C using platinum electrodes. Pt paste obtained from Ma TecK Germany was applied on both surfaces of pellets and after that the pellets were heated at 600°C in air for 4h to remove the organic binders. The complex impedance was measured at different signal frequencies ranging from 0.1Hz to 10 MHz using a Solartron SI 1260 impedance analyzer. The impedance response was studied in the temperature range 100°C to 600°C. These measurements were performed at temperature interval of 25°C; each temperature was kept constant with an accuracy of ±5°C during the measurement. Sufficient stabilization time was ensured at each particular temperature. The data analysis was done by using Z-view frequency response analyzer.

III. RESULTS AND DISCUSSION

Structural Studies

The XRD patterns obtained for all NiO$_x$-GDC$_{(1-x)}$ nanocomposite samples were compared with the JCPDS files of NiO (78-0643; cubic NiO) and GDC10 (75-0161). The XRD study has been already reported in our previous report [10]. From the XRD patterns, the lattice parameter 'a1' and 'a2' for NiO and GDC respectively was calculated using the relation,

$$a = d\sqrt{h^2 + k^2 + l^2} \tag{1}$$

The variation of lattice parameters 'a1' and 'a2' with NiO content was studied and it is shown in Fig. 1. From Fig. 1 it is observed that there is no deviation in both lattice parameters from the reported values, 5.418Å for GDC and 4.179Å for NiO.

Density Measurements

X-ray density of individual phases was calculated by using the formula,

$$\rho_x = \frac{4M}{Na^3} \tag{2}$$

Where, M is the molecular weight,
a is the lattice parameter, and
N is the Avogadro's number.
Similarly X-ray density of nanocomposite samples was calculated by using the formula,

$$\rho_{composite} = \frac{M1 + M2}{V1 + V2} \tag{3}$$

Where,
M1 = (1-x) × (Molecular weight of GDC)
M2 = x × (Molecular weight of NiO)
V1= M1 / ρx1 and V2 = M2 / ρx2
and ρx1 and ρx2 are X-ray density of GDC and NiO, respectively.

The X-ray density of the all nanocomposite samples calculated using equation (3) is tabulated in Table I. Experimental density of all the samples was calculated by Archimedes principle. It is more appropriate technique for the determination of density of porous materials. It is seen from the table that both X-ray and actual density decrease with an increase in NiO content. The results were used to estimate percentage porosity tabulated in Table I.
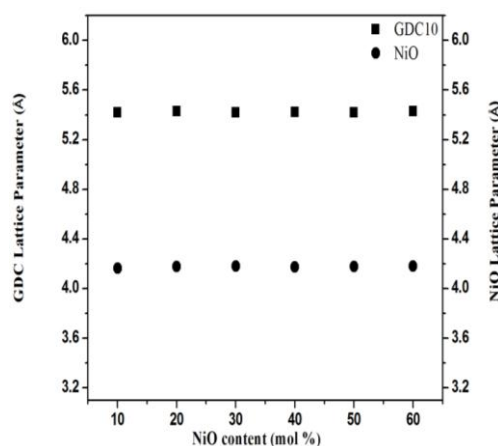

Fig. 1 Variation of lattice parameters with NiO content.

Impedance spectroscopy

The mechanism of the composite electrodes has been illustrated by Zhao *et al.* [14] and it can also be applied to the NiO-GDC nano-composites prepared in this study. They

applied two phase composite model and percolating model. According to the two-phase composite model, both e⁻ and O²⁻ transfer can be achieved respectively through continuous networks formed by NiO and GDC. While in the percolating model, the TPBs must be electrochemically active through the percolation of the ionic and electronic phases to the bulk electron and ion conductors at either end of the interface. In cermet, there is large amount of TPB regions. The ionic phase and percolating metal oxide phase provide continuous paths (two phase composite model) from TPBs to the bulk gas, whereas electronic and ionic phases (percolating model), enable these TPBs to remain active, where redox reaction is considerably enhanced.

The NiO-GDC composite is a heterogeneous composite. The two phases in this composite have different electrical conductivities. The NiO is electron conducting (p-type semiconducting) while GDC is ion conducting. Therefore, their ac conductivities are presumed to be affected by NiO content, which is studied with impedance spectroscopy.

The impedance spectroscopy is an efficient tool to resolve the contribution from various microscopic elements such as the grain, grain boundary, and electrodes to the total conductivity response. Cole-Cole and Bode representation of impedance effectively probes the series or additive processes. The Cole - Cole representation of impedance data is the plot of real part of impedance (Z') verses negative of imaginary part (Z''). It is also called as Nyquist plot. It depicts the series or additive processes in solids such as non-depletive grain resistance (R_g) and depletive grain boundary resistance (R_{gb}) for ion transport [15] i.e. total resistance (R_t) of the material at the given temperature is,

$$R_t = R_g + R_{gb} \qquad (4)$$

The Nyquist plots of all composites were recorded in the temperature range of 100°C to 600°C and are shown in Fig.2 and 3.
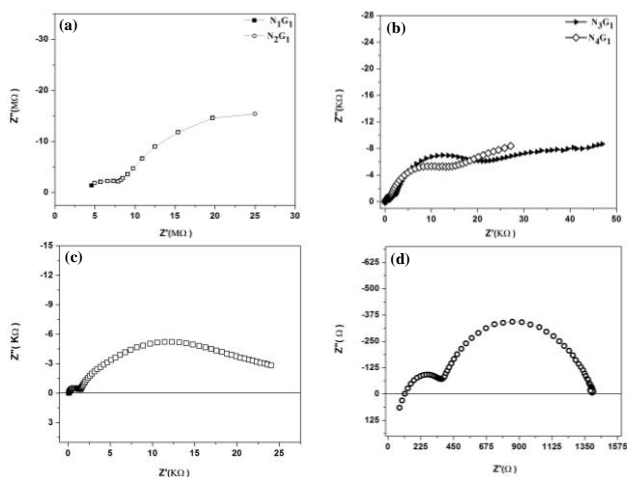

Fig. 2 Nyquist plots of (a) N1G1, N2G1 (b) N3G1, N4G1 (c) N5G1 and (d) N6G1 at 200°C.

The best fitting result of the impedance spectra for all six samples was achieved with the equivalent circuit of L1 (R1CPE1) (R2CPE2) as shown in Fig. 3(d), indicating at least two different electrode processes corresponding to high- and low-frequency arcs. The first loop contains resistance (R1)corresponding to grain (bulk) resistance and grain capacitance (CPE1) and the second loop contains resistance

corresponding grain boundary resistance (R2) and grain boundary capacitance (CPE2). CPE is a non- intuitive circuit element that represents the responses of real-world systems, and it has been proposed to explain a number of phenomena on the basis of the common thread that there exist some distributions of some physical properties in the heterogeneous system [16]. It is the constant phase element with minimum chi square value. The inductances of the circuits, L, may be the result of the Pt current/voltage probes or the high-frequency phase shift of the electrochemical equipment.

The diameter of the semicircles was found to decrease with increase in NiO content in the nanocomposite. This shows that the bulk as well as grain boundary and hence the total resistance decrease with increase in NiO content. As NiO content increases, the grain growth of GDC is retarded and results into decreased grain size whilst number of NiO grains which are more conducting is increased. This results into increased grain conductivity. The grain is more resistive than the grain boundary for GDC rich composites (N1G1 and N2G1) while the grain boundary is more resistive than the grain for NiO content ≥ 30 mol%. Similar studies by Park *et al.* [9] carried out on NiO-YSZ composites showed that upto 40 mol % NiO content, $R_{gb} > R_g$ and for higher NiO content $R_g > R_{gb}$. The dissimilarity is due to difference in particles size of the starting materials used in this work [10] and that reported in [9]-[10], [16]-[17].The less resistive grains are, obviously, attributable to nano-sized grains.

From Fig. 2 it can be observed that in the low temperature region, the composites N1G1 to N4G1 have spike at low frequency which is due to electrode polarization. On the contrary, the composites N5G1 and N6G1 showed no spike. This predicts that the electrode response is merely due to
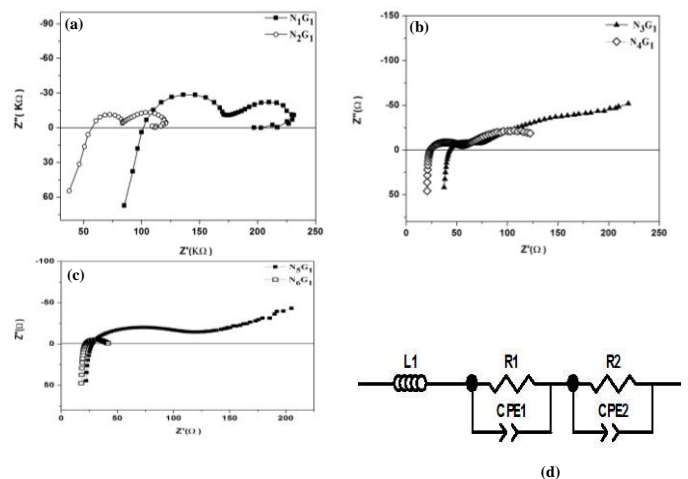

Fig. 3 Nyquist plots of (a) N1G1and N2G1 (b) N3G1 and N4G1 (c) N5G1 and N6G1 at 475°C (d) Equivalent circuit employed for evaluating the grain and grain boundary resistance.

GDC/Pt interface upto 40% NiO, which is changed to NiO/Pt interface above 40 mol% NiO i.e. for NiO rich composites. Thus negligible electrode resistance is observed for NiO/Pt and hence no electrode response is observed. 375°C the inductive loop is observed, for N1G1 and N2G1, at lower frequencies. So far the nature of these inductivities is not well understood and only some rough explanations have been given. This inductive loop may be due to impedance arising from the chemical species segregated along the grain

boundaries [18]. But as this loop appears above 375°C, very similar to the presence of electrode contribution at higher temperatures, more likely it is due to the accumulation of adsorbed species at the interface of electrode (here Pt) and sample. With increasing NiO content in the composites, the inductive loop is not observed anymore in the investigated frequency range of Nyquist plot.

Fig. 3 shows that the low frequency tail starts to appear above 475°C in case of N5G1 and N6G1. This ascertains that the main charge carriers at high temperature are the oxygen vacancies of GDC, while at low temperature, the charge carriers are electron hole pairs of NiO [9].

Further the grain boundary arc was depressed; indicative of coexistence of several processes with different relaxation times. This distribution of relaxation processes might be due to different ionic species and mechanisms involved in charge transport. Variation of Z" with frequency (f) at temperature 200°C for all the samples has been shown in Fig. 4a and 4b, which helps to probe the relaxation processes.

The relaxation time is related to the response of the charge carriers to an applied ac field. The relaxation time is defined as,

$$\tau = \frac{1}{\omega} = \frac{1}{2\pi f} \tag{5}$$

Where f is the relaxation frequency that corresponds to the maximum of the peak [19] and τ represents the mean time between two consecutive jumps of oxygen ion vacancies and it is computed from peak frequency obtained from Fig. 4a and 4b.

Relaxation processes corresponding to both grain boundary and bulk were present but the relaxation peaks were not sharp indicating non-Debye type behavior.

A loss peak observed in all the curves at high frequency region may be due to the interfacial polarization at a particular frequency range for each bulk composite. With increasing
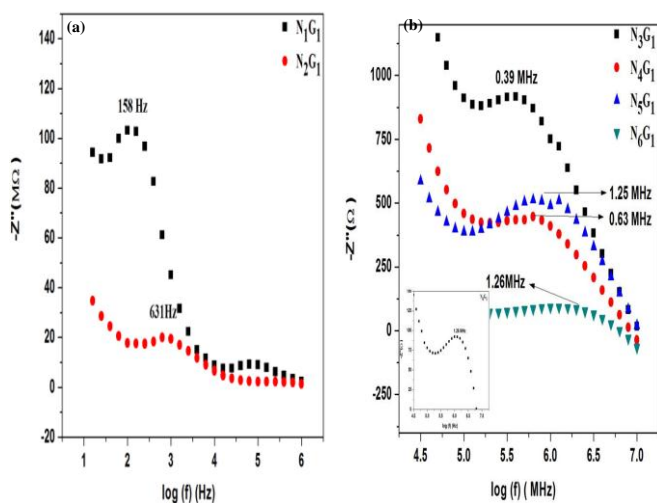
Table I Variation of density, activation energy (Ea) and relaxation time (τ) with NiO content.

Sample Name	Density		Activation Energy (eV)		Relaxat-ion Time at 200°C (μS)
	X-ray Density (gm/cc)	Experimental Density (%)	Grain	Grain Boundary	
N1G1	7.20	94.05	0.88	1.25	1.59
N2G1	7.16	93.48	0.74	0.75	1.00
N3G1	7.12	92.32	0.69	0.64	0.40
N4G1	7.07	91.30	0.61	0.76	0.25
N5G1	7.03	88.82	0.59	0.75	0.12
N6G1	6.99	86.84	0.45	0.68	0.10

NiO content, the relaxation peak shifts towards the higher frequency side. More and more free charges may accumulate on the interface resulting in a decrease of relaxation time [20]. It also shows that the height of the peak decreases with the NiO content as relaxation time decreases (Table I). Temperature dependence of relaxation frequency was also studied for nano-composites in-particular. It was observed that the relaxation peak shifts to higher frequency with rise in temperature, which is due to reduction in the time constant (RC) of the relaxation associated with both inter and intra grain charge transport, indicative of thermally activated process. This leads to successive flattening of the relaxation peaks.

The dependence of the total electrical conductivity σ (T) on NiO content, shown in Fig.5, reveals that increasing semiconductor content has a strong effect on the transport properties of the composite. This also shows that increasing NiO content results in large magnitudes of σ(T) and that such a feature is much more pronounced at low temperatures (T $\leq$ 300°C). This pronounced increase of σ (T) is related to the increasing electronic charge carriers with increasing NiO content and indicates that the percolation threshold is achieved at 40 mol % of NiO in agreement with the previous results [10]. So analogous to the results in [10], the studied compositions were identified in three different NiO concentration regions as (i) < 20 mol % of NiO (ii) 30-40 mol% of NiO (iii) $\geq$ 50 mol % of NiO. These regions indicate that distinct transport mechanism takes place depending on the NiO content. In region (i) the main charge carriers are the oxygen ions, for further increase in the NiO content (region (ii)), mixed conduction process is more likely to occur, and in region (iii) the main charge carriers may be the electron holes of NiO and GDC10 grains act as insulating scattering centers.

Assuming that these oxides exhibit polaronic conduction in the temperature range 100-500°C which is governed by a small polaron hopping mechanism,

Fig. 4 (a) Variation of –Z" with logarithmic frequency at 200°C for N1G1 and N2G1. (b) Variation of –Z" with logarithmic frequency at 200°C for samples N3G1 to N6G1; Inset: magnified view for sample N6G1.

$$\sigma = \frac{A}{T} \exp\left(\frac{-E_A}{kT}\right) \tag{6}$$

The plot of ln (σ*T) vs 1000/T (Fig. 6), called as Arrhenius plot, shows linear relationship, validating above assumption [21]-[22]. Basically there are two regions in the Arrhenius

plot, which may be due to dominance of electronic and ionic charge transport mechanism in the nanocomposite samples at different temperature regions. At high temperatures, the
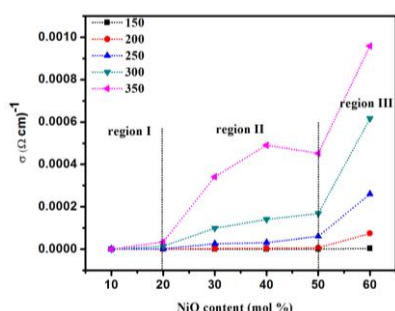

Fig. 5 Dependence of electrical conductivity on NiO content at different temperatures.
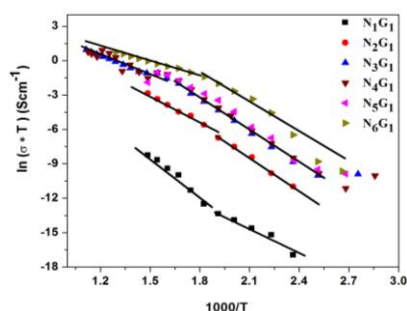

Fig.6 Arrhenius plots for N1G1 to N6G1 in the temperature range 200-600°C.

nano-composites with NiO content $\geq$ 40 mol%, showed almost same conductivity. This again supports that the main charge carriers at high temperature are the oxygen vacancies of GDC 10 whose concentration decrease with NiO content. The GDC 10 grains act as insulating scattering centers to inhibit the conductivity rise [23]. Moreover, the presence of a resistive impurity segregated at grain boundaries also contributes to the total conductivity, though not to the bulk conductivity. The activation energies of the grain (E_g) and grain boundary conductivity (E_{gb}) with varying NiO content are tabulated in the Table. I. The activation energy E_g for 10 % NiO is 0.88 smaller than 1.00 eV reported for GDC [24]-[25]. This E_g value decreased gradually for further additions of NiO and it is 0.45 eV for 60 % NiO content. This is evidently due to increased NiO grains contributing the grain conductivity. On the contrary, E_{gb} value quickly decreased from 1.25 for 10 % NiO to 0.75 eV for 20 % NiO.

For low NiO content, composite presents a system where NiO grains are segregated along the grain boundaries of GDC but with increase in NiO content, presumably, both grains get distributed along the grain boundary of their counterparts. This ultimately provides large number of GDC-NiO contacts and hence major contribution to grain boundary comes from GDC-NiO contacts although contribution from homo-grains (NiO-NiO and GDC-GDC) and porosity is also expected. Therefore, E_{gb} value also decrease with varying NiO content. In fact, for increased NiO content GDC 10 grains act as insulating scattering centers and hence the E_{gb} value increase to some extent.

IV. CONCLUSION

Electrical nano-composites of NiO_x-$GDC_{(1-x)}$ were successfully prepared by mixing combustion synthesized nano-powders. All nano-composites were found to be well crystalline with no solid solution among the constituent phases. Crystallite size of these samples was in the range of 20-26 nm. Density measurement showed decrease in density with increase in NiO content. The electrical properties of NiO-GDC nano-composites were studied for the entire composition range of composites by using impedance spectroscopy. It was evidenced from the ac impedance spectra that the grain was more resistive than the grain boundary for low NiO content while reverse was true for high NiO content. The total conductivity results manifested that the transport mechanism has changed from oxygen vacancies of GDC to electron holes of NiO with increase in NiO content. This was corroborated by the fact that at high temperatures, the nano-composites with NiO content $\geq$ 40 mol% showed almost same conductivity. The activation energies for grain and grain boundary conduction were decreased with NiO content. The electrical conductivity and activation energy showed percolative behavior with 40 mol % NiO composition. The relaxation studies showed that processes corresponding to both grain and grain boundary were present. Further, it revealed that the relaxation time decreased with both NiO content and the temperature.

REFERENCES

[1] Philippe Knauth, Harry L. Tuller, "Solid-State Ionics: Roots, Status, and Future Prospects" J. Am. Ceram. Soc., 85 [7]1654–80(2002).

[2] A. Verma, S. Basu, "Power from hydrogen and fuel cell", July, 177-181 (2005) Chemical Weekly.

[3] V. B. Tare and J. B. Wagner, "Electrical conductivity in two phase nickel–nickel oxide mixtures and conductivity of nickel oxide at the nickel–nickel oxide phase boundary" J. Appl. Phys.1983,54, 6459-6462.

[4] C. C. Liang, A. V. Joshi, N.E. Hamilton, "Solid-state storage batteries", J. Appl. Electrochemistry 8 (1978) 445-454.

[5] A. Menne, W. Wepppner, "Redox Reaction Mechanisms at the Agcl/Chlorine Gas Interface", Electrochim. Acta 1823 (1991) 11-12.

[6] N. Q. Minh, "Ceramic fuel cells", J. Am. Ceram. Soc. 76 (1993) 563-588.

[7] T. E. Mady, J. T. Yates, Jr. D. R. Scndstrom, R. J. H. Voorhoeve, in: N. B. Hannay (1976) (Ed.), Treatise on Solid state Chemistry, Vol. 6B, Plenum Press, New York, p.1

[8] Z. Wu, M. Liu, "Modelling of ambipolar transport properties of composite mixed ionic-electronic conductors", Solid State Ionics 93(1997) 65-84.

[9] Young Min Park, Gyeong Man Choi, "Microstructure and electrical properties of YSZ–NiO composites", Solid State Ionics 120 (1999) 265–274.

[10] A.U. Chavan, L.D. Jadhav, A.P. Jamale, S.P. Patil, C.H. Bhosale, S.R. Bharadwaj, P.S. Patil, "Effect of variation of NiO on properties of NiO/GDC (gadolinium doped ceria) nano-composites" Ceramics International, 38 (2012) 3191-3196.

[11] L.D. Jadhav, M.G. Chourashiya, K.M. Subhedar, A.K. Tyagi, J.Y. Patil, "Synthesis of nanocrystalline Gd doped ceria by combustion technique", J. Alloys Compd. 470 (2009) 383-386.

[12] L.D. Jadhav, M.G. Chourashiya, A. P. Jamale, A. U. Chavan, S. P. Patil, "Synthesis and Characterization of nanocrystalline Ce1-xGdxO2-x/2, (x= 0-0.30) solid solutions", J. Alloys Compd. 506 (2010) 739-744.

[13] Shaowu Zha, William Rauch, Meilin Liu, "Ni-Ce0.9Gd0.1O1.95 anode for GDC electrolyte-based low-temperature SOFCs", Solid State Ionics 166 (2004) 241–250.

[14]]Yufeng Zhao, Ding-Bang Xiong, Haiying Qin, Faming Gao, Haruyuki Inui, Bin Zhu, "Nanocomposite electrode materials for low temperature solid oxide fuel cells using the ceria carbonate composite electrolytes", International journal of hydrogen energy, 37 (2012) 19351-19356.

[15] Evgenij Barsoukov, J. Ross Macdonald," Impedance spectroscopy theory, experiment, and applications" Second Edition, A John Wiley & Sons, Inc., Publication (2005).

[16] Hongfang Zhang, Chee-Leung Mak, "Impedance spectroscopic characterization of fine-grained magnetoelectric Pb (Zr0.53Ti0.47) O3–(Ni0.5Zn0.5) Fe2O4 ceramic composites", Journal of Alloys and Compounds 513 (2012) 165– 171.

[17] Chin-Yi Chen, Yang-Ru Lyu, "Effect of NiO addition on properties of bulk yttria-doped ceria sintered from their spray pyrolyzed powder", Ceramics International 38 (2012) 3291–3300.

[18] Doreen Thiele, Andreas Zuttel, "Electrochemical characterisation of air electrodes based on La0.6Sr0.4CoO3 and carbon nanotubes", Journal of Power Sources, 183 (2008) 590–594.

[19] Rajeev Joshi, R. Mishra, S. H. Pawar, "Relaxation studies of spray deposited Bi2Co0.1V0.9O5.35 solid electrolyte thin films on stainless steel substrate" Ionics (2009) 15:453-458.

[20] J. Zhang, M. Mine, D. Zhu, and M. Matsuo, "Electrical and dielectric behaviors and their origins in the three-dimensional polyvinyl alcohol/MWCNT composites with low percolation threshold", Carbon 47 (2009) 1311.

[21] Shu-en Hou, Jose Antonio Alonso, Shreyas Rajasekhara, Marıa Jesus Martınez-Lope, Marıa Teresa Fernandez-Dıaz, John B. Goodenough , "Defective Ni Perovskites as Cathode Materials in Intermediate-Temperature Solid-Oxide Fuel Cells: A Structure-Properties Correlation", Chemistry of Materials 22(2010) 1071-1079.

[22] M.G. Chourashiya, L.D. Jadhav, "Synthesis and characterization of 10%Gd doped ceria (GDC) deposited on NiO-GDC anode-grade-ceramic substrate as half cell for IT-SOFC" International Journal of Hydrogen Energy 36 (2011) 1498-14995.

[23] V. Esposito, D. Z. de Florio, F. C. Fonseca, E. N. S. Muccillo, R. Muccillo, e. Traversa, " Electrical properties of YSZ/NiO composites prepared by a liquid mixture technique", J. European Ceramic Society 25 (2005) 2637-2641.

[24] Frank Tietz, Francisco J. Dias, Dimitris Simwonis, Detlev StoÈ ver, "Evaluation of commercial nickel oxide powders for components in solid oxide fuel cells", Journal of the European Ceramic Society 20 (2000) 1023-1034.

[25] Q.Jeangros, A.Faes, J.B.Wagner, T.W.Hansen, U.Aschauer, J.Vanherle, A.Hessler-Wyser, R.E.Dunin-Borkowski, "In situ redox cycle of a nickel–YSZ fuel cell anode in an environmental transmission electron microscope", Acta Materialia, 58 (2010) 4578-4589.

Dr. Archana Chavan is currently working as a "Postdoctoral Fellow" at Chonnam National University, South Korea. She joined the University of Johannesburg (UJ), South Africa, as a post-doctoral research fellow in 2014. Dr. Chavan received her PhD from Shivaji University, Kolhapur, India, in 2013 in physics. Her research interest is focused on the chemical synthesis of nanostructured materials and their applications in energy storage and conversion devices and sensor technology.

Dr. L. D. Jadhav is currently working as an Assistant Professor at Department of Physics, Rajaram College Kolhapur, Maharashtra, India. She was Principal Investigator (P.I.) of BRNS funded project and currently she is P.I. of Defense Research and Development Organization (DRDO) project. Total 3 Ph.D. students completed their degree and currently there are 5 students are working under her guidance for Ph.D. Her research interest is focused on the synthesis of nanostructured materials and their applications in SOFCs and batteries.

Dr. Salil Varma is currently working as a Scientist-F at Chemistry Division, Bhabha Atomic Research Centre, Trombay, Mumbai - 400085, INDIA. His research interest is focused on the synthesis of catalyst materials and their applications in SOFCs.

Prof. S. R. Bharadwaj is currently working as a Senior Scientist Chemistry Division, Bhabha Atomic Research Centre, Trombay, Mumbai - 400085, INDIA. Her research interest is focused on the synthesis of catalyst materials, ceramic materials and their applications in SOFCs and electrolysis.